ELSEVIER

Biophysical Chemistry 104 (2003) 429–447

Biophysical Chemistry

www.elsevier.com/locate/bpc

Protonation of deoxycytidine residues in dC_4 tetraloops: UV spectrophotometric study of dC_{10} and $d(A_{14}C_4T_{14})$

E. Raukas*, K. Kooli

Institute of Experimental Biology, Estonian Agricultural University, Harku 76902, Estonia

Received 18 September 2002; received in revised form 6 January 2003; accepted 22 January 2003

Abstract

It is shown that component analysis could be applied to study the UV difference spectra of cytidine oligomers and hairpin oligonucleotides with cytidines in the loop region in order to account for the melting and titration results in terms of cytidine stacking and protonation. Upon acid titration, the dC_{10} oligomer undergoes cooperative conformational transition at pH 6.3 accompanied by protonation and formation of the *i*-structure with half of the residues protonated. The stability of the hemiprotonated structure increases with decreasing pH, the *i*-structure persisting still in the region of $pH < pK$ of cytidine. An UV difference spectrum that reflects the stacking/unstacking of hemiprotonated cytidine residues was acquired from the melting and titration experiments of the dC_{10} oligomer and used to describe the behavior of the dC_4 loop of the hairpin oligonucleotide $d(A_{14}C_4T_{14})$. It is shown that upon titration, the 50% level of protonation of the deoxycytidine tetraloop is attained at pH 5.0. Simultaneously, the stacking interactions of cytidine residues reach the maximum at this pH with two residues stacked, and thereafter decline again. Only marginal stabilization of the oligomer hairpin ($\Delta T_m = 1.5$ °C) is found to accompany the formation of this single hemiprotonated $dC{\cdot}dC^+$ base pair. We propose that at pH 5 the cytidines of the dC_4 loop form a hemiprotonated $dC{\cdot}dC^+$ pair stacked with the last $dA{\cdot}dT$ base pair of the hairpin stem.

Keywords: Oligonucleotide; Acid titration; T_m; Cytidine protonation; UV difference spectra; Spectral component analysis

1. Introduction

One of the remarkable features of DNA is its structural polymorphism. A large variety of DNA conformations have been found in recent years, including the *Z*-form, triple helix, tetraplex, *i*-form etc., that all cover a number of different H-bond networks between bases. Under appropriate conditions, the formation of looped out regions and hairpin structures among other non-canonical forms of DNA, though rare, may possibly play an important role in gene control mechanisms. These single-stranded regions of DNA could be connected with a possible presence of cruciform structures and arise in single stranded DNA of filamentous phages as well.

Spectroscopic methods have been commonly used to study the thermodynamic parameters of helix–coil transition of the DNA and RNA oligo-

*Corresponding author. Tel.: +372-6560615; fax: +372-6506091.

E-mail address: ergo@ebi.ee (E. Raukas).

0301-4622/03/$ - see front matter © 2003 Elsevier Science B.V. All rights reserved.
doi:10.1016/S0301-4622(03)00032-2

mers. In order to get the thermodynamic data, absorbance at a single wavelength has been monitored as a function of temperature. Thus, in difference from CD spectra the rich information content of the whole UV spectrum is neglected entirely. Several other analytical methods have been used to evaluate the thermodynamic parameters of melting of the duplexes and hairpins based on a silent assumption that the transition describes a two-state process. Occasionally, this assumption has turned out to be erroneous and been possibly avoided by multi-wavelength methods. Single wavelength UV melting curves are commonly used to evaluate the effects of mispairing, presence of unpaired residues and loops. On the contrary, a whole range of UV spectral data is hardly used to study the conformation of the loop residues, to give an example. At the same time, all constituents of nucleic acids have distinctive UV spectra and, therefore, could be followed individually.

We have made use of both the titration and thermal UV difference spectra to study the conformation of dC-containing oligonucleotides in acidic conditions. We will show that the spectra of these oligonucleotides can be described in terms of base stacking and protonation as a function of pH and temperature.

The structure of different hairpin loops of DNA oligonucleotides has been extensively studied in vitro [1,2]. In most cases, the loops consisting of four nucleotides are found to be the most stable. In the same solvent conditions there are no large differences in stability between the loops of dA_n, dT_n, dG_n and dC_n, the dT_n loop being marginally more stable than the rest [3–5]. Interactions in the loop region can significantly contribute to the overall stability of the hairpin. Substitution of all four dT residues of the hairpin loop by difluorotoluene residues increases the stability of the oligomer by 10.8 °C upon thermal denaturation, due to the increased stacking in the loop region [6].

X-Ray, NMR and molecular mechanics have been used to study the loop structures. There is a general tendency for self-complementary sequences to crystallize as duplexes even in presence of destabilizing mispairing in the central part of the oligomers that complicates the X-ray studies of the hairpin structures. As a rule, pseudo-infinite helices are formed in crystals by end-to-end stacking; in other cases quite peculiar structures are occasionally found in the end regions of the oligomers. Data concerning the loop conformation have, therefore, been mostly acquired on the basis of NMR experiments.

The DNA hairpin loops similar to RNA hairpin loops could be well ordered. However, the structures of only a few DNA hairpins have been elucidated up to now, e.g. [7–10]. Several detailed studies of the dT_4 loop structure have been made [7,11–15] whereas there are no data concerning the structure of the cytidine tetraloops except for the loop of the parallel stranded DNA duplex [16] and rC_4 loop [17–19].

2. Methods

2.1. Biochemicals

Oligonucleotides $d(A_nC_4T_n)$ ($n=12$, 14) were synthesized on a DNA synthesizer Expedite PerSeptive Biosystems, Model 8909. Poly-(dA)·poly(dT) and dC_{10} were obtained from Sigma; rC_{10} was a gift from V.I. Yamkovoi (Novosibirsk State University).

2.2. Buffers and solutions

The buffer for the titration and melting experiments used in the region pH 7–5 was 10 mM sodium cacodylate containing 200 mM NaCl and 0.1 mM EDTA (CN buffer). When titration was extended below pH 5.0, a composite buffer was applied for the same experiments containing an additional 10 mM succinate (CSN buffer). The strand concentrations were determined from absorbance values at 80 °C using the following molar extinction coefficients (M^{-1} cm^{-1}): $\varepsilon_{260}(dA)=15\,400$, $\varepsilon_{260}(dT)=8800$, $\varepsilon_{260}(dG)=11\,700$, $\varepsilon_{260}(dC)=7300$. The concentrations are always expressed as the total concentration of phosphate residues, $c=[P^-]$.

2.3. UV measurements

The UV spectral measurements were performed with Pye-Unicam SP8-150 spectrophotometer. The

instrument was interfaced with a PC equipped with homemade software for reading the digitized results and performing a variety of operations (smoothing, shifting, light scattering corrections, calculation of derivatives and differences, etc.). Single beam mode was applied using the concentration scale of the instrument (four decimal places) yielding the results in 10^{-4} optical density (OD) units. Up to 10 readings were averaged at each point. All measurements were made against air, except the titration experiments that were performed against the buffer in reference beam. The acquired spectra and obtained melting fine structure curves were not corrected for the temperature dependent change of the solution volume.

2.4. Thermal denaturation

The complexes were prepared by annealing the solutions before the experiments. The solutions were heated to 80 °C and allowed to cool slowly overnight. Fine structure of melting was measured at 260 nm for every 0.1 °C at a rate of 0.8 °C min^{-1} by using ultrathermostat U1 (MLW Prüfgeräte-Werk, Medingen). Special custom-made thermostated cell holders were used with the temperature sensor placed directly in the 1-cm pathlength Teflon-stoppered cell. The readings were taken in time intervals of approximately 1 s and averaged digitally. Absorbance was measured against air and corrected for a small increase in buffer absorbance upon temperature registered earlier. Melting temperatures were derived by computer fitting of theoretical model (all-or-none process) [20].

2.5. Titration

To avoid possible minor contamination, the titration was performed directly in 1-cm cuvettes and measured against the buffer solution in the reference beam. The predetermined amounts of 0.4 M HCl were added with microsyringe to both cuvettes (maximally up to 100 μl). The pH of the buffer solution was calibrated in advance using digital pH meter OP-211/1 (Radelkis). The final values of pH were checked and compared with the value expected on the basis of calibration. The spectra were measured in 1-nm steps and corrected for the dilution and occasional small baseline shifts (referenced to A_{320}). After appropriate corrections, the difference spectra against pH 7.0 were calculated and digital data at eight wavelengths transferred to component analysis program. The experimental data were thereafter interpolated with a step of 0.25 pH units making use of cubic polynomial fitting through five neighboring experimental points.

2.6. Component analysis

The fractions of spectral components (f_{kj}) were derived from the following system of linear equations [21]:

$$\Delta A_{ij} = \beta_{ik} \times f_{kj}, \quad (1)$$

hence

$$f_{kj} = (\beta_{ki} \times \beta_{ik})^{-1} \times (\beta_{ki} \times \Delta A_{ij}), \quad (2)$$

Here, k ($k=1$, 2, and in some cases, 3) refers to a respective component (cytidine protonation, stacking/unstacking of cytidine residues, etc.), i stands for the wavelength ($i=1$–8) and j for the pH or temperature value (in titration and melting experiments, respectively). Occasionally, the presence of other components was tested for, (e.g. denaturation of dA·dT base pairs by making use of poly(dA)·poly(dT) thermal denaturation spectrum as a reference, thermal perturbation spectrum of cytidine, etc.).

ΔA_{ij} is the matrix of absorbance differences registered upon titration or melting and is used after appropriate interpolation. β_{ki} is a matrix of spectral coefficients found from respective molar coefficients. Cytidine protonation spectrum on a molar basis ($\Delta\varepsilon_i^+$) was used [22] whereas the basic difference spectrum of hemiprotonated cytidine stacking ($\Delta\varepsilon_i^=$) was found as described in Section 3. The coefficients β_{ki} were found from respective molar spectra $\Delta\varepsilon_{ki}$ using:

$$\beta_{ki} = \Delta\varepsilon_{ki} \times c \times b_{k,} \quad (3)$$

where c stands for concentration $[P^-]$ and the relative content of a given type of the nucleotide in the oligomer is given by b_k ($b_k=0-1$). The set of eight wavelengths i used routinely was 255–290 nm with the step of 5 nm. The absorbance as well as respective temperature values were registered during the steady increase of temperature. An average of 10 readings at each wavelength was registered. It follows that the measurements at different wavelengths were made at slightly different temperatures. To get uniform results at different wavelengths, the data from thermal denaturation experiments were interpolated with the step of 1 °C.

Standard deviations Δf_{kj} were found using the covariant matrix [23]:

$$\Delta f_{kj}=\sqrt{\sigma_{kj}^2}, \tag{4}$$

where σ_{kj} are the diagonal elements of the matrix

$$D(f_j)_{kk}=\sigma_j^2\ (\beta_{ki}\times\beta_{ik})^{-1}. \tag{5}$$

In turn, the dispersion σ_j was found from diagonal elements of the covariant matrix

$$D(\Delta A)_{ij}=\frac{\left(\Delta A_{ij}^{\exp}-\sum_k \beta_{ik}f_{kj}\right)^{-1}\cdot\left(\Delta A_{ij}^{\exp}-\sum_k \beta_{ik}f_{kj}\right)}{i-k} \tag{6}$$

where i ($i=1-8$) and k ($k=2$ or 3) are the number of wavelengths and spectral components, respectively. Overall accuracy of the experiment was estimated according to the expression [21]:

$$R=\frac{\sum_i\sum_j\left(\Delta A_{ij}^{\exp}-\sum_k \beta_{ik}f_{kj}\right)^2}{\sum_i\sum_j(\Delta A_{ij}^{\exp})^2}. \tag{7}$$

3. Results

3.1. Determination of stacking/unstacking difference spectrum of hemiprotonated form of $dC\cdot dC^+$

Acid titration as well as the thermal denaturation of dC_{10} results in a complex picture of UV spectral changes associated with protonation (or deprotonation) of cytidine residues and conformational transitions of the oligomer (Figs. 1 and 2).

The difference spectra of acid titration for a wavelength range used in component analysis of the present study are depicted in Fig. 1. The isosbest of the titration curves (273 nm) does not coincide with the expected isosbest of cytidine protonation at 265 nm. It follows that the curves are not due to the cytidine protonation solely, the most probable explanation of the observed shift being the concomitant change in stacking interactions of the cytidine residues.

In order to use the component analysis to describe the titration in terms of (i) conformation of the oligomer and (ii) protonation, the respective portion of the difference spectrum caused by stacking of cytidines ($\Delta A_i^=$) must be elucidated. The component analysis presumes the additivity of partial difference spectra:

$$\Delta A_i^{\exp}=\Delta A_i^+ + \Delta A_i^=. \tag{8}$$

Here subscript i refers to the wavelength and superscripts + and = stand for the protonation and stacking, respectively. The difference spectrum caused by the cytidine unstacking ($\Delta A_i^= > 0$) could be found from the experimental difference spectrum of melting ($\Delta A_i^{\exp}$) under the acidic conditions after appropriate correction to the presence of protonated cytidine (ΔA_i^+). As a matter of accuracy, the respective experiment was performed at pH 2.86, distant enough from the pK of the cytidine (pK 4.3 at 20 °C). At this pH the value of cytidine protonation is: (i) close to 100% [exact value is found from Eq. (10)]; and (ii) relatively unsensitive in respect to inaccuracy or occasional change of pH. We have used for calculations the value of cytidine protonation pK 3.89 at 80 °C [24]. ΔA_i^+ is found on the basis of tabulated values

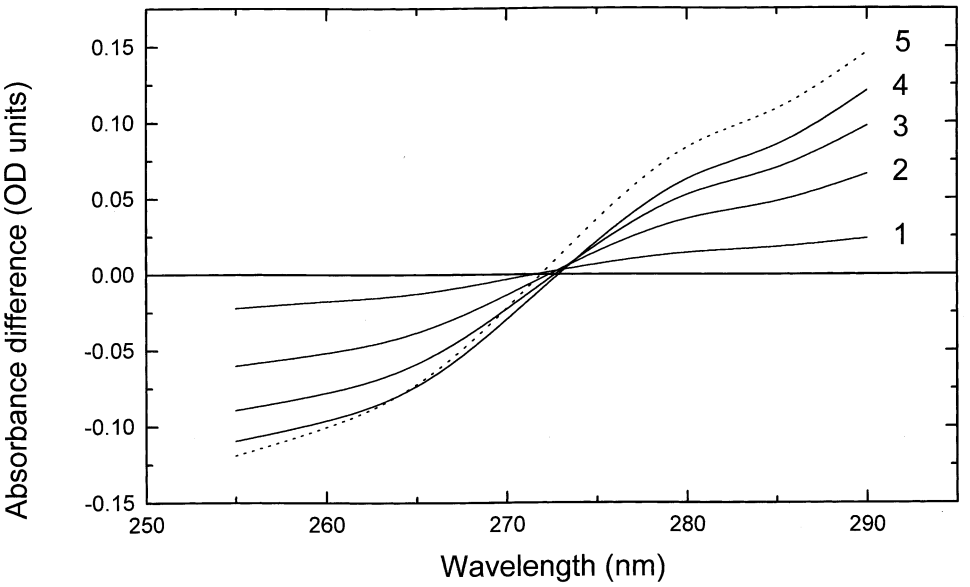

Fig. 1. Titration difference spectra of dC_{10} ($c = 0.477.10^{-4}$ M) in CSN buffer (10 mM cacodylate, 10 mM succinate, 200 mM NaCl and 0.1 mM EDTA) at 20 °C with respect to the spectrum at pH 7.0: (1) pH 6.50, (2) pH 6.25, (3) pH 6.00, (4) pH 5.75 and (5) pH 3.75 (dashed line).

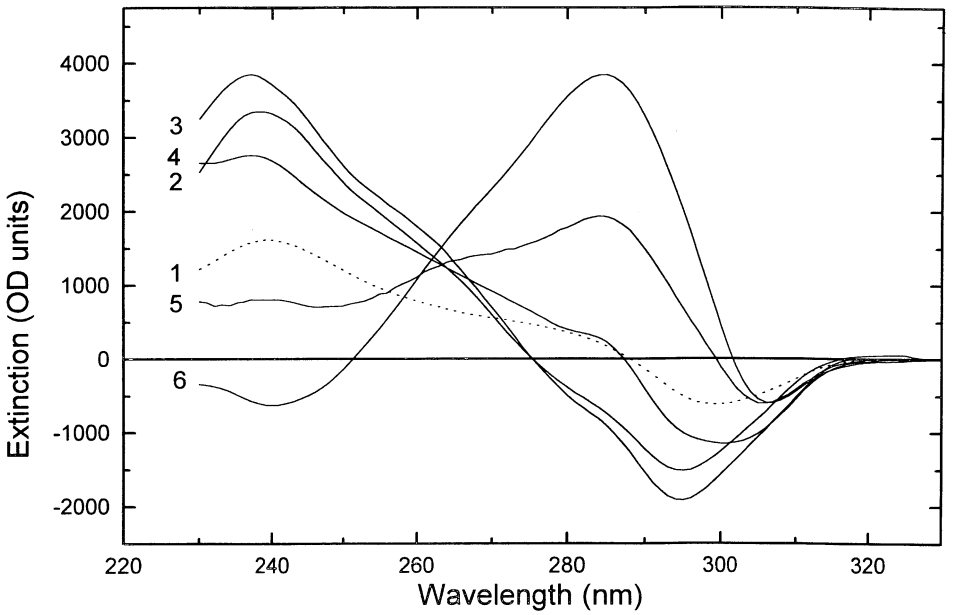

Fig. 2. Temperature difference spectra of dC_{10} between 15 and 85 °C at the following values of pH in CSN buffer, (1) first melting at pH 7.00, (2) pH 6.30, (3) pH 5.80, (4) pH 4.60, (5) pH 3.68 and (6) pH 3.24.

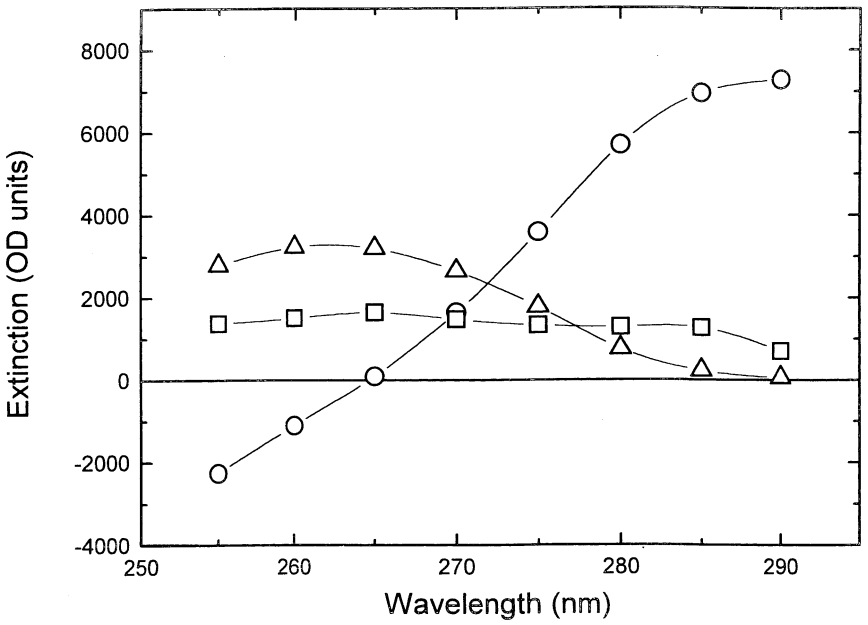

Fig. 3. Molar difference spectra of dC protonation ($\Delta\varepsilon^{+}$) (○), unstacking of hemiprotonated dC_{10} ($\Delta\varepsilon^{=}$) (□) and temperature denaturation spectrum of poly(dA) poly(dT) (Δ). The respective absorbance values at eight wavelengths were used as cofficients β_{ik} (Eq. (3)) to calculate the fractions of protonated cytidines and stacking of hemiprotonated dC·dC^{+} base pairs. Experimental difference spectra are approximated by a sum of the first and second spectra taken in respective proportions (see Fig. 6).

of cytidine protonation spectrum ($\Delta\varepsilon_i^{+}$), the expected concentration of protonated cytidine residues (c^{+}), pK of cytidine monophosphate and pH value of the given melting experiment:

$$\Delta A_i^{+} = \Delta\varepsilon_i^{+} \times c^{+}, \tag{9}$$

$$c^{+} = \frac{c}{1+10^{pH-pK}}. \tag{10}$$

Thus, the respective partial difference spectrum produced by the stacking of hemiprotonated deoxycytidines could be expressed as follows:

$$\Delta A_i^{=} = \Delta A_i^{exp} - \Delta\varepsilon_i^{+}\frac{c}{1+10^{pH-pK}}. \tag{11}$$

The resulting partial difference spectrum on a molar basis is shown in Fig. 3 together with the cytidine protonation spectrum. These two spectra were used as basis spectra for the component analysis.

It must be mentioned that the stacking spectrum of the cytidine residues could not be obtained from measurements at pH 7 (Fig. 2, curve 1). The first measurement of the denaturation spectrum of a fresh specimen of dC_{10} at pH 7 yields a spectrum similar to the denaturation spectra in acidic region with a low degree of protonation. However, repeated measurements of the same specimen at pH 7 result in a different type of spectrum which did not lend itself for the further analyses on the basis of cytidine protonation, thermal perturbation spectra [24–26], stacking spectrum of hemiprotonated cytidine or otherwise.

In case of rC_{10} the thermal difference spectra both at pH 7.0 and pH 2.7 were used beside the protonation spectrum.

3.2. Titration and thermal melting of dC_{10}

Titration curves in terms of the cytidine protonation and stacking were calculated by making use of the component analysis. The same basis spectra

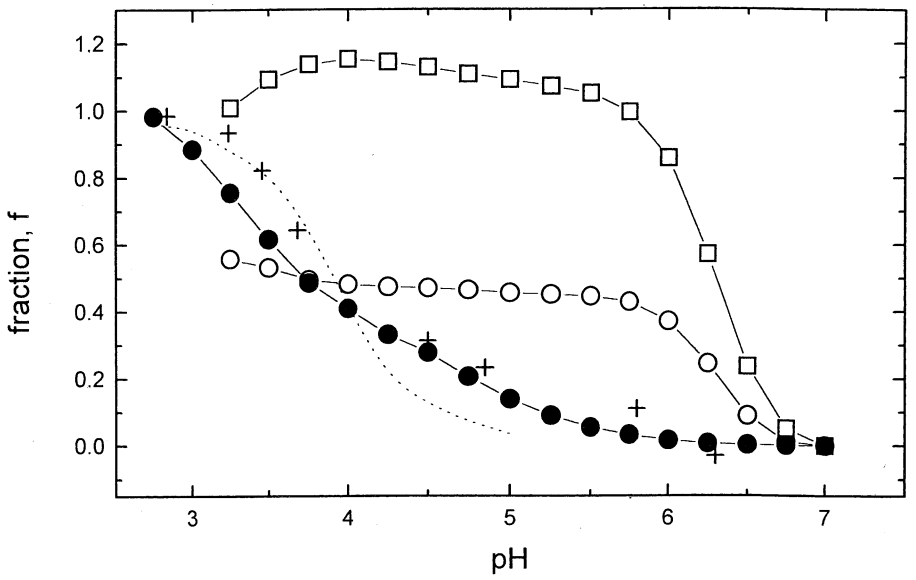

Fig. 4. Protonation and changes in the base stacking at 20 °C in the course of acid titration of dC_{10} and rC_{10} as calculated according to Eq. (2). Protonation of dC_{10} ($R=18\%$) and rC_{10} ($R=0.06\%$), (○) and (●), respectively, formation of a secondary structure by hemiprotonated dC_{10} residues (*i*-structure) in the course of acid titration (□), fraction of protonated dC^+ residues at 85 °C as a function of pH, i.e. the sum of respective titration and melting experiments [Eq. (12)] (+). Dashed line indicates the expected degree of protonation for a dC monomer (p*K* 3.9 assumed). The root mean square deviations of the protonation and stacking of the dC_{10} and rC_{10} titration curves at pH 4.0 and 3.0 are (± 0.007, ± 0.011) and (± 0.010, ± 0.016), respectively.

(Fig. 3) were used to calculate both the titration and melting curves of dC_{10} at different pH values. The results of the component analysis of acid titration spectra are presented in Fig. 4. A cooperative transition between pH 6.75 and 5.75 with the midpoint at pH 6.3 can be seen. The protonation levels off at approximately $f^+=0.5$ and thus half of the dC residues remain unprotonated in the region below pH 5.75. The curve depicting the stacking of $dC{\cdot}dC^+$ base pair parallels well with the protonation curve for the decreasing pH values between pH 7.0 and pH 5.75 up to $f^{=}\approx 1.0$ as expected.

In the region of pH 3.5–5.5 the value of $f^{=}$ is approximately 1.1–1.2. However, the calibration of the scale to account for stacking is quite arbitrary. In our case, the value $f^{=}=1.0$ is assigned to the state of the cytidine stacking in dC_{10} oligomer at pH 2.86, 80 °C; $f^{=}=0$ at 15 °C pH 7. Therefore, it is not unexpected to find the relative value of stacking in this region ranging from 1.1 to1.2.

At lower values (pH < 4), a gradual increase of protonation takes place, coupled with a decrease in the degree of stacking. However, a mismatch between the experimental and calculated values remains small. Standard errors at the end of the dC_{10} titration curve are $\Delta f^+=\pm 0.007$, $\Delta f^{=}=\pm 0.010$ and $\Delta f^+=\pm 0.021$, $\Delta f^{=}=\pm 0.032$ at pH 4.5 and pH 3.5, respectively (Fig. 4). The same is true for the overall error *R*. It means that the partial difference spectrum of stacking, derived from the titration data, and the partial spectrum used to treat the melting data of the same specimen are close to each other (apart from the sign) in the measured pH range. This result was expected. The 50% protonated ($f^+=0.5$) and highly stacked ($f^{=}=1.0$) structure could be considered as a stable conformational state of the dC_{10} oligomer in the region of pH 5.7–3.5.

The results of the melting experiments at pH 4.85 and pH 2.86 are presented in Fig. 5 as curves of the components f^+ and $f^{=}$. Experimental points labeled by crosses in Fig. 4 correspond to resultant

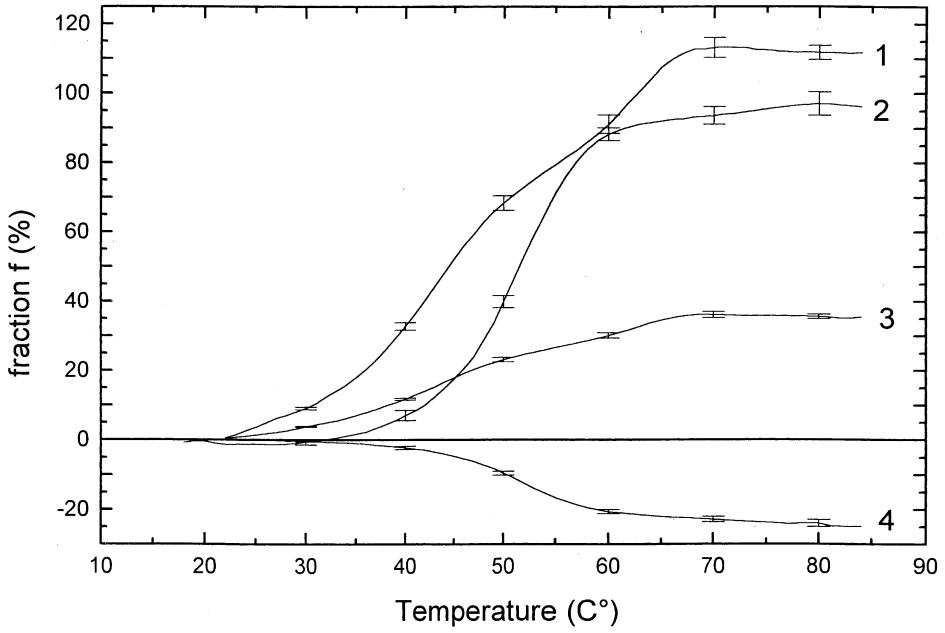

Fig. 5. Melting of dC_{10} at pH 2.86 (curves 1 and 3, $c=0.180\times10^{-4}$, $R=0.09\%$) and pH 4.85 (curves 2 and 4, $c=0.225\times10^{-4}$, $R=0.54\%$). Curves 1 and 2 depict the unstacking of dC residues (results not normalized) whereas curves 3 and 4 correspond to the respective change in the degree of protonation. If pH < pK (pH 2.86), the degree of protonation increases in the course of melting. The opposite takes place at pH 4.85. In both cases, the breakdown of the secondary structure is nearly complete ($f\cong1.00$). Vertical lines are shown every 10 °C to indicate the standard error (Eq. (4)).

values of the protonation due to titration (f^+_{pH}) and thermal denaturation ($f^+_{T_m}$) at a particular pH value (at 85 °C):

$$f^+ = f^+_{pH} + f^+_{T_m}, \quad (12)$$

$f^+_{T_m}$ can be either negative (pH > pK) or positive (pH < pK). As a result, the values of f^+ at the end of melting curves are expected to approach those of dC monomer protonation. It can be seen (Fig. 5) that at pH 2.86 the dissociation of the hemiprotonated dC·dC$^+$ base pairs is accompanied by the binding of additional protons ($f^+_{T_m}>0$). On the other hand, at pH 4.85, melting is accompanied by the release of protons ($f^+_{T_m}<0$). For pH < pK, the values of cytidine protonation at the end of the melting curve (Fig. 4) fit the curve of cytidine protonation for pK 3.9. However, in the range pH > pK, the protonation values for 85 °C do not follow the theoretical curve of protonation for a given pK, indicating that the reversal of the hemiprotonated form upon melting is not complete. Fitting of the spectra for all cases of the melting and titration experiments yield rather good results (Fig. 6a–d).

One must bear in mind that both the pK of the cytidines, and the pH of the buffer solution depend upon temperature and thus tend to change during the melting. As a result, the overall behavior of the system is quite complex and does not allow a straightforward and exact approach. The pK of the cytidine-5′-phosphate in the solution with an ionic strength of 0.2 (Na^+) shifts from 4.50 at 10 °C to 3.89 at 80 °C [24] whereas the change of buffer pH is opposite in direction and it is difficult to draw conclusive inferences concerning the exact values of the parameters involved.

Upon titration, the rC_{10} oligomers yield difference spectra with isosbest at shorter wavelengths (258 nm) as compared with isosbest of dC_{10} at 272 nm, on the other side of the isosbest of cytidine protonation (265 nm). The difference

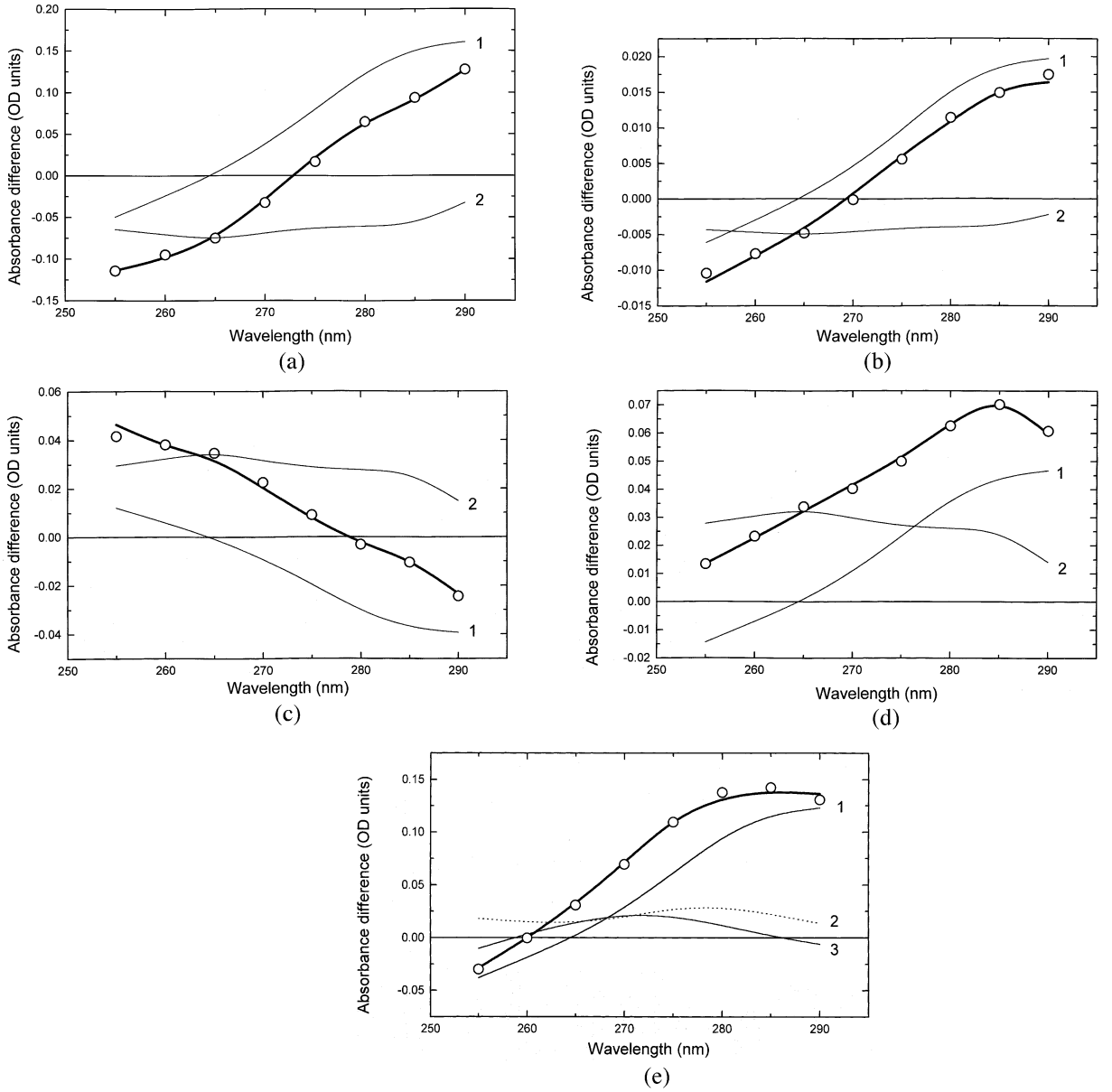

Fig. 6. Spectral components of titration and of the melting experiments of dC_{10} (a, c, d), rC_{10} (e) and $d(A_{12}C_4T_{12})$ (b) in the following conditions: (a) titration at pH 5.5 against pH 7.0, 20 °C, $c=0.477\times10^{-4}$ M, (b) titration of $d(A_{12}C_4T_{12})$ at pH 5.0, 20 °C, $c=0.366\times10^{-4}$ M, (c) melting at pH 4.85, 80 °C, $c=0.225\times10^{-4}$ M, (d) melting at pH 2.86, 80 °C, $c=0.180\times10^{-4}$ M, (e) titration of rC_{10} at pH 2.75, 20 °C, $c=0.358\times10^{-4}$ M. The components are dC protonation (f^{+}, curves 1) and stacking/unstacking of hemiprotonated $dC{\cdot}dC^{+}$ base pairs ($f^{=}$, curves 2), as found by the least square fitting according to Eq. (2) (see Section 2). In the case of rC_{10}, the curve (2) depicts the part of the spectrum due to the decay of structure characteristic for pH 7 whereas curve (3) is a spectrum characteristic of the structure formed in acid (thermal denaturation spectrum at pH 2.7 with opposite sign). Solid line depicts experimental data, circles show calculated values of absorbance (sum of all components).

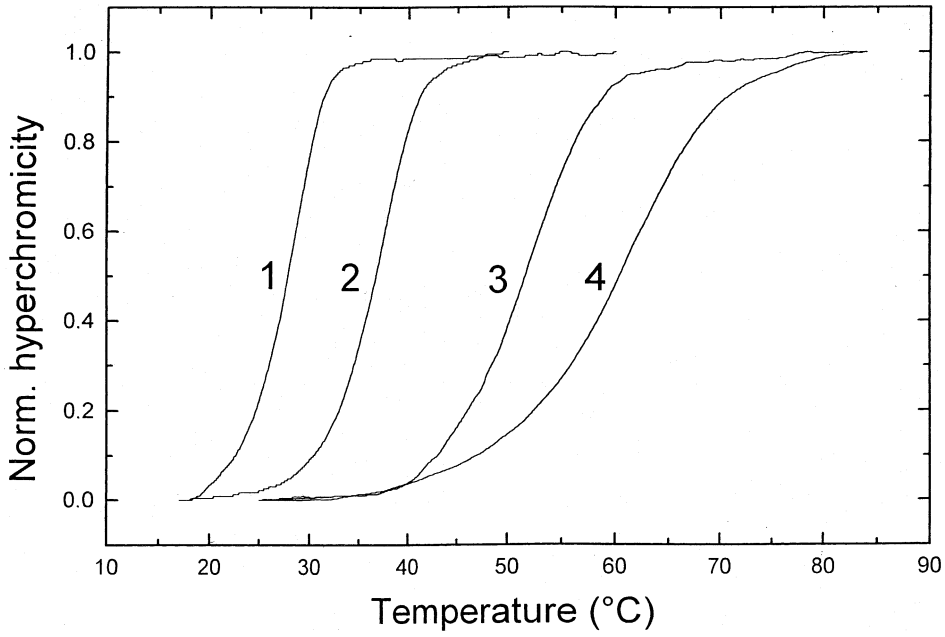

Fig. 7. Melting of dC_{10} at 260 nm in CSN buffer at the following pH values: (1) 6.3, (2) 5.8, (3) 5.0 and (4) 3.7.

spectrum of rC_{10} titration permits perfect approximation by component analysis ($R=0.06\%$) if along with protonation spectrum the thermal denaturation spectra both at pH 2.7 (with opposite sign, i.e. respective to formation of another type of stacking upon titration) and pH 7.0 are used for calculations (Fig. 6e, components 1–3).

3.3. Melting temperatures of dC_{10}

The melting curves of dC_{10} as a function of pH are depicted in Fig. 7. The stability of the acid form of dC_{10} increases drastically as pH decreases and drops in the region $pH<pK$. T_m increases from 27.9 °C at pH 6.3 to 60.6 °C at pH 3.7 with the hyperchromicity at 260 nm of approximately 30%. Occasionally, the melting curves in acidic conditions have been found to consist of two steps (Fig. 5 curve 1, see also [27]).

Melting of the fresh specimen at pH 7.0 yields a very sharp transition with $T_m=35.2$ °C and hyperchromicity at 260 nm of just 11.5%. It is not possible to resolve the difference spectrum of this transition into two or more components in a satisfactory manner, similar to that of the melting and titration experiments at $pH<7.0$. The second melting of the same specimen results in only a small decline of absorbance at 260 nm and the weak difference spectrum of the second melting is quite different (not shown).

3.4. Protonation and stacking interactions in the dC_4 hairpin loop

In general, acid titration of $d(A_{14}C_4T_{14})$ results in a difference spectrum similar to dC_{10} spectrum in the same conditions. The isosbest is again found at 272 nm instead of 265 nm in the pH region from pH 7.0 to 5.0. From this point on, the isosbest gradually shifts towards that of the cytidine protonation at 265 nm. There is no absorbance increase in the spectral region 260–270 nm which could be associated with the denaturation of dA·dT base pairs (Fig. 3). Therefore, the difference spectrum could be totally attributed to the changes taking place in the dC_4 loop of the hairpin. When component spectra derived from experiments with dC_{10} are used to describe the changes taking place

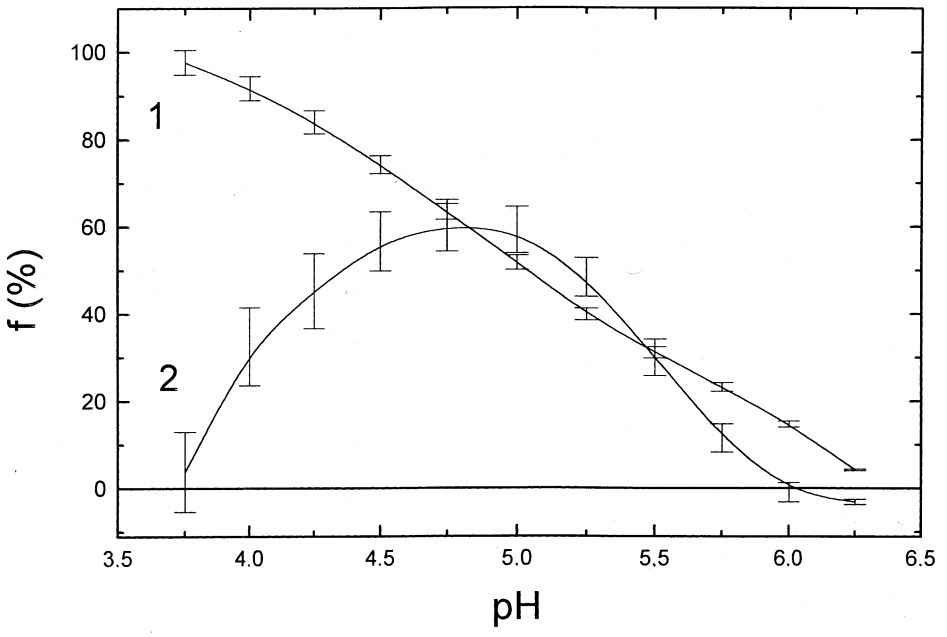

Fig. 8. Protonation and changes in the base stacking at 20 °C in the course of acid titration of d($A_{12}C_4T_{12}$), $c = 0.366 \times 10^{-4}$, $R =$ 0.47%. (1) f^+, Protonation, (2) $f^=$, stacking of hemiprotonated cytidine bases. Vertical lines depict the standard error. See Fig. 6b for the component spectra at pH 5.0.

in the loop, the fits of the difference spectra are rather good (Fig. 6b). This means that the difference spectra are fully understood in terms of the protonation/deprotonation and stacking/unstacking taking place in the loop region. The stacking of cytidine residues ($f^=$) reaches maximum at approximately pH 5 (Fig. 8) when more than 50% of cytidines are protonated. The increase of stability of the oligomer in the region of approximately pH 5 is marginal and does not exceed 1.5 °C (Fig. 9). When calculated against pH 5, the isosbest shifts further toward shorter wavelengths upon titration and a subsequent calculations at pH $<$ 3.5 making use of component analysis requires definitely more than two components to be considered. A further decrease of pH results in a gradual drop of T_m, possibly due to the protonation of adenines.

4. Discussion

4.1. Method

The method of component analysis has been successfully used as early as in 1960s for calculating the melting curves separately for dA·dT and dG·dC base pairs of DNA [21,28–30] making use of the averaged molar extinction coefficients for hyperchromic spectra of base pairs as deduced from the analysis of DNAs of different base compositions. On the contrary, determination of the nucleotide composition of the DNA and RNA specimens as well as nucleotide mixtures based upon the least square analysis of UV spectra [31–33] has not found common application in a laboratory practice. The method allows one also to follow the dissociation and migration of ligands during the thermal denaturation on the background hyperchromic spectrum of dA·dT and dG·dC base pairs [34]. The method has been occasionally used to decompose the hyperchromic spectra of triple helices into components describing the dissociation of the third strand and duplexes in case of dC×dG·dC [35] and U×A·U [36]. Although the produced empirical spectra are rather averaged and rough by nature, quite reasonable base pair dissociation curves have been reported.

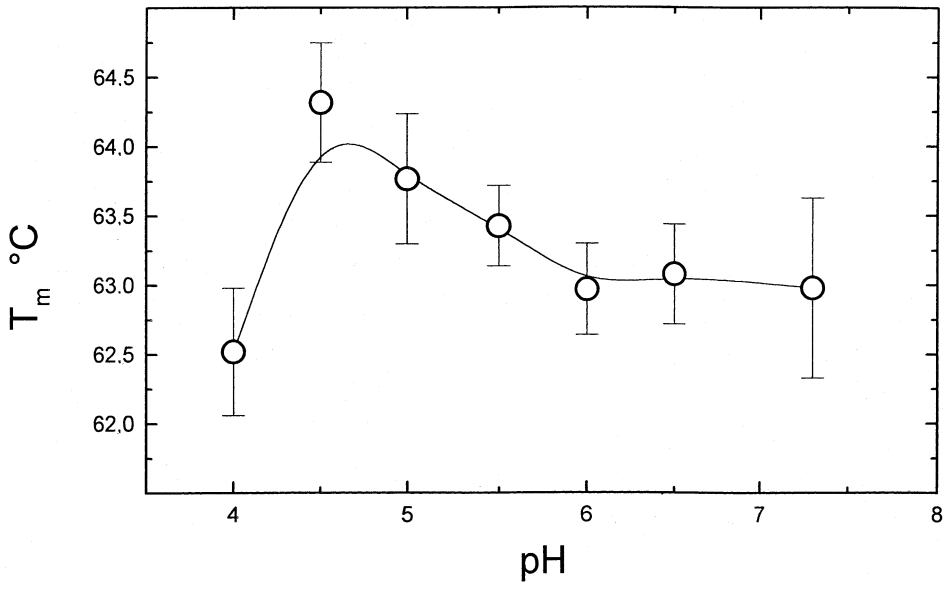

Fig. 9. Melting temperature of the hairpin duplex d($A_{14}C_4T_{14}$) as a function of pH in CSN buffer.

A more detailed examination of the denaturation spectra reveals at least four–five significant component species even in case of simple deoxypolynucleotides [37]. At the same time, this increase in number of components includes small and often similar in shape contributions and results in the marked increase of standard deviation of the curves. Therefore, we had not used more than three components in our practice. In principle, also the dependence of absorbance by mononucleotides upon temperature due to the concomitant change of hydration [24–26] must be considered. However, the correction is not very large and can be neglected.

On the other hand, the titration and melting experiments have been occasionally performed at several wavelengths without further treatment of the data [22,38]. It allows one to distinguish the main characteristics of different processes simultaneously taking place in the same specimen. Inevitably, the respective results are merely qualitative.

The protonation of cytidine, unlike to the protonation of adenosine, can be easily followed because of its large difference spectrum [22]. The results of our analysis of the deoxycytidine decamer in the pH region of 7.0–4.0 allow us to conclude that acid titration and melting of this oligomer could be satisfactory described in terms of protonation and stacking interactions of hemiprotonated cytidine residues, i.e. these spectra are additive. The fit of the experimental spectra by the sum of the components is rather good (Fig. 6a–d) and thus, the difference spectra of cytidine oligomers can be described as a sum of conformational and protonation terms.

The stability of dA·dT base pairs in a broad range of pH allows to expect that the same two spectral components related to the dC residues of the hairpin loop of d($A_{12}C_4T_{12}$) could be distinguished without the interference from the denaturation of helical stem. Indeed, it turned out that the part of the difference spectrum related to dC (affected by both pH and temperature) is readily visible on the dense background of absorbance of 12 dA·dT base pairs (Fig. 6b).

4.2. Structure of cytidine oligomers dC_{10} in acid

In case of single-stranded oligomers containing three or more sequential cytidines, a four-stranded hemiprotonated structure forms as demonstrated

first by Gehring on the bases of the NMR spectrum of $d(TC_5)$ [39]. Determinations of structures by X-ray analysis and NMR followed for dC_4 [40], $d(C_3T)$ [41] and several other oligomers. The formation of quadruplexes (tetramers in case of dC_n oligomers) at acid pH has been shown to be a rather general phenomenon inherent to different cytidine oligomers [42,43]. The structure was shown to be stable between pH 6 and pH 3 [42]) with an optimum of thermal stability for dC_5 at pH 4.5 as determined by the amplitude of the CD spectra at 288 nm [44]. The cytidine oligomers (or oligomers containing the stretches of cytidines) form a parallel-stranded duplex with $dC{\cdot}dC^+$ pairs and two such duplexes associate head-to-tail by base pair intercalation into a quadruplex [43]. In all cases, four-stranded complexes were found held together by intercalated $dC{\cdot}dC^+$ base pairs.

From our titration experiments it is concluded that in a weak acid oligomer dC_{10} readily attains a secondary structure, which is characterized by both a large hypochromic change and protonation of 50% of cytidine residues (Fig. 4). This structure is stable at least up to pH 3.5. Essentially, the two components, i.e. the cytidine protonation and stacking of hemiprotonated cytidine residues, completely account for the experimental difference spectrum (Fig. 6a). The relative increases and decreases of the components' magnitude upon both titration and melting are strictly parallel to each other. The concurrent change of the components is in good agreement with the idea of formation and decay of a single type of structure.

As a rule, we found the melting curves of the acidic structure of dC_{10} consisting of a single cooperative transition, in difference from earlier reports [45] where two or more steps were observed in the melting curves of dC_8 at pH 5. Occasional appearance of multiple melting transitions in the acid region, (e.g. Fig. 5, curves 1 and 3) could be explained by the presence of different multiplexes [27]. This means that the formation of secondary structure in principle does not necessarily yield *i*-form (tetramers $[dC_{10}]_4$) only. However, annealing greatly increases the presence of *i*-form. Formation of other non-equilibrial structures (duplexes, octamers) can be possibly taking place during the rapid change of pH in titration

However, titration curves strongly suggest of the presence of a single kind of structure. In addition, the constancy of isosbest in every single melting experiment allows us to state that all these structures (if present) have a great deal in common: (i) the hemiprotonation of cytidines; and (ii) the similar type of stacking geometry. Moreover, in experiments only annealed specimens were used. It is, therefore, deduced that under the present experimental conditions the dC_{10} oligomer predominantly attains a conformation known as *i*-form.

4.3. Structure of cytidine oligomers rC_{10} in acid

The cooperative behavior of dC_{10} is in contrast with that of respective RNA oligomer rC_{10} under the same conditions. Upon acid titration at 20 °C, the protonation of rC_{10} in our experiments starts at pH 6 and follows thereafter around the protonation values of the respective DNA oligomer at 85 °C (Fig. 4). In both cases, the protonation in the pH region of 4.0–5.0 is somewhat higher than expected on the basis of p*K* of cytidine alone, which allows one to suppose that some interactions give rise to the phenomenon. No cooperative transition could be detected for rC_{10} in accordance with earlier reports for different ribocytidine containing oligomers [46].

The titration curve of rC_{10} is clearly different from the one obtained in titration experiments with poly(rC) [47,48] which is thought to form a double-stranded structure $poly(rC){\cdot}poly(rC^+)$ at acidic pH values [49]. The cooperative transition

$$2poly(rC) \rightarrow poly(rC){\cdot}poly(rC^+)$$

depends slightly on the ionic strength and takes place in the region of pH 5.0–6.3 [47,48]. The respective value of p*K* of the $(rC){\cdot}(rC^+)$ double helix varies from approximately 5.9 at $[Na^+] = 1.0$ M to approximately 5.4 at $[Na^+] = 0.01$ M [48,50,51], whereas for the corresponding DNA polymer p*K* 7.2 was found [51], independent of ionic strength. In contrast, melting temperature of the double-stranded $(rC){\cdot}(rC^+)$ polymer [52] as well as dC_{10} in our experiments essentially depend on pH and the ionic strength of the solution.

Considering the above we conclude that the rC_{10} oligomer, unlike the respective polymer in earlier reports [47–51] does not form any kind of a hemiprotonated multi-stranded structure.

The different behavior of dC_{10} and rC_{10} can possibly be explained by the presence of some kind of specific structure in rC_{10} at pH 7 and room temperature. The structure of a single stranded poly(rC) has been considered by Arnott [53,54] and found to be a six-fold helix, in difference of dC_{10} residual double helix under the same conditions (similar to the structure in acid). The hyperchromic spectrum of rC_{10} at pH 7 has two maxima at $\Delta\varepsilon_{279}=1590$ and $\Delta\varepsilon_{279}=1380$; hyperchromic spectrum of dC_{10} is depicted in Fig. 2 (curve 1).

4.4. Structure of hairpin loops

Majority of research on DNA hairpins has been focused on thymidine loops of various sizes. The optimal size of dT_n loop is determined to be 3–5 bases [5,11–15,55–59]. The same is true for different RNA loops [19]). The presence of the dT tetraloop stabilizes the hairpin by an enthalpic contribution of approximately 5–7 kcal/mol when compared to the respective duplex [11,56,60,61].

The DNA loop consisting of only two thymidine residues could be formed. The evidence for this statement comes from the following observations. When dA residue is introduced into the last position of the dT tetraloop, a dA·dT pair is readily formed, properly leaving the two central dT residues as a loop [8,12]. Also, the tetraloop d(GTTA) forms a dG·dA non-canonical base pair, stacking partially with the last base pair of the stem and leaving the two thymidine residues in the form of a loop [62]. The first one of them stacks upon its 5′-neighboring dG and the second points the solvent. A hairpin loop of only two nucleotides d(GT) may bridge the minor groove of the DNA double helix without any major readjustment of the last dG·dC base pair [63,64]. A loop consisting of two thymidine residues was observed in case of a mixed quadruplex–triplex structure connecting the Watson–Crick dG·dC pair of the triad dA×dG·dC [65]. Molecular dynamics calculations demonstrate that a loop consisting of a single dT residue results in a buckling of the last dG·dC pair of the stem [66]. One concludes that in order to form a stable loop, two residues are required as a minimum.

The dT tetraloop is highly structured. It has been shown by NMR studies and molecular mechanical calculations that the imino protons of the first and last thymidine residues of the hairpin tetraloop are directed towards each other and stack over the last base pair of the stem [7,9,12]. However, the results concerning the conformation of the second and third dT residues of the loop vary. According to the model proposed by Hare [7] for the oligonucleotide d(CGCGTTTTCGCG), the 5′-strand of the stem is extended by a stack of the first residue of the loop T5 over the residue G4. Residues T7 and T8 extend the 3′-strand of the stem, the last residue located upon the C9. The second residue of the loop (T6) connects the ends of these two stacks and thus makes the turn of the chain.

According to the model presented by Haasnoot and Hilbers [9,11,12,67], the stacking characteristic for the DNA B-form continues from the 5′-end of the oligomer d(ATCCTATTTTTAGGAT) up to the third base of the loop (T9). A sharp turn of the sugar-phosphate backbone follows in order to connect the fourth dT residue of the loop (T10), which stacks over the T11 residue of the stem. As a result, the stacking continues after the 5′-end of the stem by three bases so that all bases are more or less turned inward of the helix. In case of type II loops, the second residue of the loop is turned into the minor groove [67,68]. NOE experiments suggest that this is true also with respect to the fourth residue which is turned inward and forms a non-canonical T7·T10 pair with the first base of the loop.

The loop structure is obviously affected by the base pair composition of the stem and a base pair adjacent to the loop [9,62,68,69]. The conformation of the same loop, (e.g. dT_4) could be different in case of different stems. The closing base pair has often been found to deviate from the canonical Watson–Crick pair. Structures of various DNA hairpin loops are discussed in reviews [1,2,9,70]. In general, the DNA stacked loops are expected to form as extensions of 5′-part of the stem whereas RNA loops form as extensions of 3′-part of the stem. Also, in case of the triple helix, the dT_4

loops are well ordered with respect to the rest of the structure and as such can contribute to the overall stability of the triplex [71].

Imino protons of thymines located in the loop region are sensitive to pH and temperature and less sensitive to salt concentration [60]. Since, in many cases, both the first and last bases of the tetraloop point inward toward each other, it is tempting to speculate that they might form a 'wobble pair'; in any case their imino protons are shown to be close in space. The last dT residues of the d(C_nT) oligomers in a four-stranded *i*-structures form a dT·dT pair [41] stacked upon the last dC·dC$^+$ pair [39].

It can be concluded that there is a general trend toward formation of H-bonded base pair between the first and last residues of the tetraloop. The same is expected to take place in case of other pyrimidine loops.

4.5. Structure of loops containing cytidine residues

Up to date there are no NMR or X-ray data regarding the structure of the cytidine loops at the end of the hairpin with antiparallel strands. The dC_4 loop structure of the parallel-stranded DNA duplex hairpin [16], the loop consisting of a single cytidine [72] as well as loops consisting of two pyrimidines d(CT) and d(TC) [73] have been described. In case of a helix with parallel dA_8 and dT_8 strands held together by the eight reverse Watson–Crick base pairs and by dC_4 tetraloop results in a stable hairpin [16]. While the hairpin loops in DNA generally require two or more residues, in the presence of the closing d(G·A) pair [72] the sheared geometry in both ends of the stem brings the sugars of G5 and A7 of the oligomer d(CAATGCAATG) close enough to be bridged by a single cytidine. The cytidine base stacks on the guanosine of the d(G·A) pair with the sugar stacked on the adenosine. In the double pyrimidine hairpins [73] the first base is loosely bound in the minor groove whereas the second base of the loop is stacked upon the helix stem.

Our results demonstrate that upon acid titration of d($A_{14}C_4T_{14}$) the cytidine residues become protonated in a broad range of pH values between 6 and 3, accompanied by the initial increase of stacking interactions (Fig. 8). The degree of stacking attains the highest level at pH 5.0–4.5 and fades gradually thereafter. Protonation of the loop cytidines of more than 1 pH unit higher than the p*K* value of the cytidine suggests the presence of some secondary structure involving the H-bonds. The protonation curve is not sigmoidal which is apparently due to different environment of the individual dC residues. The experiments were performed in conditions favorable for hairpin formation: (i) low oligonucleotide concentrations were used (as a rule, $A_{260} < 0.1$ OD); and (ii) complexes were annealed before each experiment.

Since it is possible to form helical loops consisting of only two pyrimidine residues, the result could be best explained assuming the formation of one hemiprotonated dC·dC$^+$ pair in the initial part of the titration curve (25% cytidines protonated at pH 5.4) stacked with the last dA·dT pair of the helical stem. Upon further protonation ($f^+ > 0.5$), the subsequent cytidines become protonated. At the same time the charge repulsion is expected to prevent the occurrence of dC$^+$·dC$^+$ base pairs coupled with the unstacking, all in good accordance with the presented experimental data. However, the overall stabilization of the hairpin seems to be small in contrast to the case of triple helix with paperclip structure that contains two dC_4 hairpin loops between the dA_{10} and both dT_{10} strands [74]. They observed the stabilization of the triplex of approximately $\Delta T_m = 7$ °C at pH 6 upon titration, compared to $\Delta T_m = 1.5$ °C stabilization at pH 5 in our case (Fig. 9).

The model proposed above to account the protonation and partial stacking of loop residues can be compared with results related to mispairings in DNA. While it is possible that the dC·dC mismatched pair is compatible with the B-form geometry of the double helix at neutral pH, the formation of dC$^+$·dC$^+$ pair is excluded due to inability to form H-bonds. The dC·dC$^+$ base pair, as it is introduced in an oligonucleotide duplex achieves its highest stability at pH 5.3 [75], is possibly formed by two H-bonds instead of a potential single bond at pH 7. The increase in stability between pH values of 7.0 and 5.3 is quite noticeable ($\Delta T_m > 10$ °C). Even larger stabilization values occurring between pH 8.4 and pH 5.2 are

reported ($\Delta T_m = 12$ °C) for another oligonucleotide duplex with the dC·dC mismatch [76]. In neutral conditions, the dC·dC mispairs adopt the wobble structure. This and other py·py type of mismatches in the DNA oligomers have a lower stacking potential at neutral pH than the pu·pu mismatches. As a result, the destabilization of the helix is more pronounced [77]. However, the NMR experiments show that dC·dC as well as dT·dT and dT·dC mismatches, although the most unfavorable ones when located in the interior of the duplex [78], are readily incorporated into the helix at neutral pH in the presence of high salt [76]. It has not been possible to propose the detailed structure of the mispair solely based on the NMR results. The anti–anti conformation of the pair was suggested on the basis of stereochemical considerations. The dC·dC mismatch is the most unfavorable among other py·py mismatches in neutral solution in the presence of 1 M NaCl [76,78,79]. In the central part of the oligomer duplex, the dT·dT mismatch yields an enhanced rate of helix opening [80]. The dC·dC mismatch in this case yields on average of 0.7 kcal/mol higher stability at pH 4.9 than that at pH 7.0 whereas the dT·dT mismatch becomes less stable by the same value.

In conclusion, the authors are of the opinion that although the pairs dC·dC or dC·dC^+ are rather weak, they can be agreed with the B-form geometry of DNA. We expect the formation of the dC·dC^+ pair between the first and the last dC residue in the dC_4 tetraloop at the end of the double helical stem with the Watson–Crick base pairs.

Acknowledgments

This work was supported by grant 3709 from Eesti Teadusfond. We wish to thank Dr H. Schütz for the d($A_{14}C_4T_{14}$) and d($A_{12}C_4T_{12}$) specimens and for the T_m calculations, Dr V.I. Yamkovoi for the specimen of rC_{10}, Marika Alter for technical assistance and Dr Ülo Vaher and H. Ivanova for advice regarding computer programs.

References

[1] D.L. Patel, L. Shapiro, D. Hare, Nuclear magnetic resonance and distance geometry studies of DNA structures in solution, Ann. Rev. Biophys. Biophys. Chem. 16 (1987) 423–454.

[2] G. Varani, Exceptionally stable nucleic acid hairpins, Ann. Rev. Biophys. Biomol. Struct. 24 (1987) 379–404.

[3] M.M. Senior, R.A. Jones, K.J. Breslauer, Influence of loop residues on the relative stabilities of DNA hairpin structures, Proc. Natl. Acad. Sci. US 85 (1987) 6242–6246.

[4] M.V. Germann, B.W. Kalisch, P. Lundberg, H.J. Vogel, J. van de Sande, Perturbation of DNA hairpins containing the *Eco*RI recognition site by hairpin loops of varying size and composition: physical (NMR and UV) and enzymatic (*Eco*RI) studies, Nucl. Acids Res. 18 (1990) 1489–1498.

[5] T.M. Paner, P.V. Riccelli, R. Owczarzy, A.S. Benight, Studies of DNA dumbbells. VI. Analysis of optical melting curves of dumbbells with a sixteen-base pair duplex stem and end-loops of variable size and sequence, Biopolymers 39 (1996) 779–793.

[6] E.T. Kool, J.C. Morales, K.M. Guckian, Mimicking the structure and function of DNA insights into DNA stability and replication, Angew. Chem. Int. Ed. 39 (2000) 990–1009.

[7] D. Hare, B.R. Reid, Three-dimensional structure of a DNA hairpin in solution: two-dimensional NMR studies and distance geometry calculations on d(CGCG-TTTTCGCG), Biochemistry 25 (2000) 5341–5350.

[8] M.J.J. Blommers, F.J.M. van de Ven, G.A. van der Marel, J.H. Ven Boom, C.W. Hilbers, The three-dimensional structure of a DNA hairpin in solution. Two-dimensional NMR studies and structural analysis of d(ATCCTATTTATAGGAT), Eur. J. Biochem. 201 (1991) 33–51.

[9] F.J.M. van de Ven, C.W. Hilbers, Nucleic acids and nuclear magnetic resonance, Eur. J. Biochem. 178 (1988) 1–38.

[10] S.-H. Chou, K.-H. Chin, C.-W. Chen, Enhanced loop DNA folding induced by thymine-CH_3 group contact and perpendicular guanine–thymine interaction, J. Biomol. NMR 19 (2001) 33–48.

[11] C.A.G. Haasnoot, C.W. Hilbers, G.A. van der Marel, J.H. van Boom, U.C. Singh, N. Pattabiraman, et al., On looping in nucleic acid hairpin-type structures, in: R.H. Sarma, M.H. Sarma (Eds.), Biomolecular Stereodynamics IV, Proceedings of the Fourth Conversion of Discipline Biomolecular Stereodynamics, Adenine Press, Albany, 1986, pp. 101–115.

[12] C.A.G. Haasnoot, M.J.J. Blommers, C.W. Hilbers, Conformational aspects of hairpin loops in DNA oligonucleotides, Structural Dynamics and Functional Biomolecules, 1st EBSA Workshop Marcus Wallenberg Symp, Saltsjöbaden, 1987, pp. 212–216.

[13] R. Chattopadhyaya, S. Ikuta, K. Grzeskowiak, R.E. Dickerson, X-Ray structure of DNA hairpin molecule, Nature 33 (1988) 175–179.

[14] R. Chattopadhyaya, K. Grzeskowiak, R.E. Dickerson, Structure of a T_4 hairpin loop on a *Z*-DNA stem and

comparison with A-RNA and B-DNA loops, J. Mol. Biol. 211 (1990) 189–210.
[15] M. Ghosh, N.V. Kumar, U. Varshney, K.V.R. Chary, Structural characterisation of a uracil containing hairpin DNA by NMR and molecular dynamics, Nucl. Acids Res. 27 (1999) 3938–3944.
[16] N. Zhou, M.W. Germann, J.H. van de Sande, N. Pattabiramann, H.J. Vogel, Solution structure of the parallel-stranded hairpin d(T8◇C4A8) as determined by two-dimensional NMR, Biochemistry 32 (1993) 646–656.
[17] J. Gralla, D.M. Crothers, Free energy of imperfect nucleic acid helices. III. Small internal loops resulting from mismatches, J. Mol. Biol. 73 (1973) 497–551; 78 (1973) 301–310.
[18] O.C. Uhlenbeck, P.N. Borer, B. Dengler, I. Tinoco, Stability of RNA hairpin loops: A_6-C_m-U_6, J. Mol. Biol. 73 (1973) 483–496.
[19] D.R. Groebe, O.C. Uhlenbeck, Characterization of RNA hairpin loop stability, Nucl. Acids Res. 16 (1988) 11725–11735.
[20] H. Schütz, E. Stutter, K. Weller, I. Petri, Design and data analysis of DNA binding experiments, Stud. Biophys. 104 (1984) 23–34.
[21] G. Felsenfeld, G. Sandeen, The dispersion of the hyperchromic effect to thermally induced transitions of ribonucleic acids, J. Mol. Biol. 5 (1962) 587–610.
[22] R.A. Cox, A possible method for characterizing the secondary structure of ribonucleic acids, Biochem. J. 100 (1966) 146–169.
[23] D. Hudson, Statistics. Geneva, 1964.
[24] A. Wróbel, A. Rabczenko, D. Shugar, Conformation of acid forms of polyC: temperature and ionic strength dependence of protonation of cytidine and cytidine-5′-phosphate, Acta Biochim. Pol. 17 (1970) 339–349.
[25] D. Frechet, R. Ehrlich, P. Remy, J. Gabarro-Arpa, Thermal perturbation differential spectra of ribonucleic acids. II Nearest neighbour interactions, Nucl. Acids Res. 7 (1979) 1981–2001.
[26] A.A. Mayevsky, Temperature dependence of electronic absorption spectra of polynucleotides and their components, Biofizika 20 (1975) 957–960.
[27] T. Rush, H.Y. Yong, W.L. Peticolas, Structure and stability of cytosine deoxyoligonucleotides multiplexes, Biopolymers 41 (1997) 121–130.
[28] H.R. Mahler, B. Kline, B.D. Mehrotra, Some observations on the hypochromism of DNA, J. Mol. Biol. 9 (1964) 801–811.
[29] H. Votavová, J. Šponar, Z. Šormová, Comparison of heterogeneity of deoxyribonucleic acids of different origin by the method of hyperchromic spectra, Coll. Czech. Chem. Comm. 33 (1968) 4356–4368.
[30] R.D. Blake, T.G.J. Hydorn, Spectral analysis for base composition of DNA undergoing melting, Biochem. Biophys. Methods 11 (1985) 307–316.
[31] S. Lee, D. McMullen, G.L. Brown, Methods for automatic nucleotide sequence analysis, Biochem. J. 94 (1965) 314–322.
[32] J.N. Toal, G.W. Rushizky, A.W. Pratt, H.A. Sober, Computer assisted characterization of oligoribonucleotides by their ultraviolet absorption, Anal. Biochem. 23 (1968) 60–71.
[33] N.J. Holness, G. Atfield, Application of a spectrophotometric method to the determination of the composition of oligonucleotides obtained from cysteine transfer ribonucleic acid, Biochem. J. 159 (1976) 15–22.
[34] E. Raukas, T. Räim, Thermal denaturation of distamycinA DNA complexes as followed by hyperchromic spectra, Biophys. Chem. 11 (1980) 233–237.
[35] L. Lavelle, J.R. Fresco, UV spectroscopic identification and thermodynamic analysis of protonated third strand deoxycytidine residues at neutrality in the triplex $d(C^+–T)_6$:$[d(A–G)_6$•$d(C–T)_6]$; evidence for a proton switch, Nucl. Acids Res. 23 (1995) 2692–2705.
[36] E. Raukas, K. Kooli, V.I. Yamkovoi, H. Schütz, Free energy of the binding of uridylic acid oligomers with double stranded poly(A)•poly(U), Biophys. Chem. 67 (1997) 245–261.
[37] I. Haq, B.Z. Chowdhry, J.B.T. Chaires, Singular value decomposition of 3-D DNA melting curves reveals complexity in the melting process, Eur. Biophys. J. and Biophys. Lett. 26 (1997) 419–426.
[38] C. Zimmer, G. Luck, H. Venner, Studies on the conformation of protonated DNA, Biopolymers 6 (1968) 563–574.
[39] K. Gehring, J.-L. Leroy, M. Guéron, A tetrameric DNA structure with protonated cytosine–cytosine base pairs, Nature 363 (1993) 561–565.
[40] L. Chen, L. Cai, X. Zhang, A. Rich, Crystal structure of a four-stranded intercalated DNA: d(C4), Biochemistry 33 (1994) 13540–13546.
[41] C.H. Kang, I. Berger, C. Lockshin, R. Moyzis, A. Rich, Crystal structure of intercalated four-stranded d(C3T) at 1.4 Å resolution, Proc. Natl. Acad. Sci. US 91 (1994) 11636–11640.
[42] J.-L. Leroy, K. Gehring, A. Kettani, M. Guéron, Acid multimers of oligodeoxycytidine strands: stoichiometry, base-pair characterization, and proton exchange properties, Biochemistry 32 (1993) 6019–6031.
[43] M. Guéron, J.-L. Leroy, The *i*-motif in nucleic acids, Current Opin. Struct. Biol. 10 (2000) 326–331.
[44] S. Robidoux, R. Klinck, K. Gehring, M.J. Damha, Association of branched oligonucleotides into the *i*-motif, J. Biomol. Struct. Dyn. 15 (1997) 517–527.
[45] D. Rohozinski, J.M. Hancock, M.A. Keniry, Polycytosine regions contained in DNA hairpin loops interact via a four-stranded, parallel structure similar to the *i*-motif, Nucl. Acids Res. 22 (1994) 4653–4659.
[46] L. Lacroix, J.-L. Mergny, J.-L. Leroy, C. Hélène, Inability of RNA to form the *i*-motif: implications for triplex formation, Biochemistry 35 (1996) 8715–8722.

[47] M.-T. Sarocchi, Y. Courtois, W. Guschlbauer, Protonated polynucleotide structures. Specific complex formation between polycytidylic acid and guanosine or guanylic acids, Eur. J. Biochem. 14 (1970) 411–421.
[48] A.I. Petrov, V.I. Suchorukov, Spectrophotometric and potentiometric study on the mechanism of protonation of polycytidylic acid, Stud. Biophys. 65 (1977) 107–119.
[49] R. Langridge, A. Rich, Molecular structure of helical polycytidylic acid, Nature 198 (1963) 725–728.
[50] D. Thiele, W. Guschlbauer, Polynucleotides protonés. VII Transitions thermiques entre differents complexes de l'acide polyinosinique et de l'acide polycytidylique en milieu acide, Biopolymers 8 (1969) 361–378.
[51] W. Guschlbauer, M. Blandin, J.L. Drocourt, M.N. Thang, Poly-2′-deoxy-2′-fluoro-cytidylic acid: enzymatic synthesis, spectroscopic characterization and interaction with poly-inosinic acid, Nucl. Acids Res. 4 (1977) 1933–1943.
[52] W. Guschlbauer, Protonated polynucleotide structures, I. The thermal denaturation of polycytidylic acid in solution, Proc. Natl. Acad. Sci. US 57 (1967) 1441–1448.
[53] S. Arnott, Secondary structure of polynucleotides, Proceedings of the 1st Cleveland Symposium on Macromolecules 1977, 87–104.
[54] A.G.W. Leslie, S. Arnott, Structure of the single-stranded polyribonucleotide poly(2′-O-methylcytidylic acid), J. Mol. Biol. 119 (1978) 399–414.
[55] C.W. Hilbers, C.A. Haasnoot, S.H. de Bruin, S.H. Joordens, G.A. van der Marel, J.H. van Boom, Hairpin formation in synthetic oligonucleotides, Biochimie 67 (1985) 685–695.
[56] C.A.G. Haasnoot, S.H. de Bruin, R.G. Berendsen, H.G.J.M. Janssen, T.J.J. Binnendijk, C.W. Hilbers, Structure, kinetics and thermodynamics of DNA hairpin fragments in solution, J. Biomol. Struct. Dyn. 1 (1983) 115–129.
[57] C.A.G. Haasnoot, S.H. de Bruin, C.W. Hilbers, G.A. van der Marel, J.H. van Boom, Loop structures in synthetic oligonucleotides. Hairpin stability and structure studied as a function of loop elongation, J. Biosci. 8 (1985) 767–780.
[58] D. Renzeperis, K. Alessi, L. Marky, Thermodynamics of DNA hairpins: contribution of loop size to hairpin stability and ethidium binding, Nucl. Acids Res. 21 (1993) 2683–2689.
[59] M. Amarathunga, E. Snowden-Ifft, D.E. Wemmer, A.S. Benight, Studies of DNA dumbbells. II Construction and characterization of DNA dumbbells with a 16 base-pair duplex stem and T_n end loops ($n=2$, 3, 4, 6, 8, 10, 14), Biopolymers 32 (1992) 865–879.
[60] S. Ikuta, R. Chattopadhyaya, H. Ito, R.E. Dickerson, D.R. Kearns, NMR study of a synthetic DNA hairpin, Biochemistry 25 (1986) 4840–4849.
[61] L.E. Xodo, G. Manzini, F. Quadrifoglio, G.A. van der Marel, J.H. van Boom, Thermodynamic behaviour of the heptadecadeoxynucleotide d(CGCGCGTTTTTCGCGCG) forming *B* and *Z* hairpins in aqueous solution, Nucl. Acids Res. 14 (1986) 5389–5398.
[62] M.J.P. van Dongen, M.M.W. Mooren, E.F.A. Willems, G.A. van der Marel, J.H. van Boom, S.S. Wijmenga, et al., Structural features of the DNA hairpin d(ATCCTA-GTTA-TAGGAT): formation of a G–A base pair in the loop, Nucl. Acids Res. 25 (1997) 1537–1547.
[63] L.P.M. Orbons, A.M. van der Gijs, J.H. van Boom, C. Altona, An NMR study of the polymorphous behavior of the mismatched DNA octamer d(m^5C-G-m^5C-G-T-G-m^5C-G) in solution. The B, Z, and hairpin forms, J. Biomol. Struct. Dyn. 4 (1987) 939–963.
[64] L.P.M. Orbons, A.A. van Beuzekom, C. Altona, Conformational and model-building studies of the hairpin form of the mismatched DNA octamer d(m^5C-G-m^5C-G-T-G-m^5C-G), J. Biomol. Struct. Dyn. 4 (1987) 965–987.
[65] H.M. Al-Hashimi, A. Majumdar, A. Gorin, A. Kettani, E. Skripkin, D.J. Patel, Field- and phage-induced dipolar couplings in a homodimeric DNA quadruplex: relative orientation of G•(C-A) triad and G-tetrad motifs and direct determination of C2 symmetry axis orientation, J. Am. Chem. Soc. 123 (2001) 633–640.
[66] S.R. Bhaumik, Conformational feasibility of a DNA hairpin with one-base loop, Biochem. Biophys. Res. Comm. 220 (1996) 853–857.
[67] M.J.P. van Dongen, S.S. Wijmenga, G.A. van der Marel, J.H. van Boom, C.W. Hilbers, The transition from a neutral-pH double helix to a low-pH triple helix induces a conformation switch in the CCCG tetraloop closing a Watson–Crick stem, J. Mol. Biol. 263 (1996) 715–729.
[68] S.-H. Chou, Y.-Y. Tseng, B.-Y. Chu, Stable formation of a pyrimidine-rich loop hairpin in a cruciform promoter, J. Mol. Biol. 292 (1999) 309–320.
[69] M.J.J. Blommers, J.A.L.I. Walters, C.A.G. Haasnoot, J.M.A. Aelen, G.A. van der Marel, J.H. van Boom, et al., Effects of base sequence on the loop folding in DNA hairpins, Biochemistry 28 (1989) 7491–7498.
[70] C.V. Hilbers, H.A. Heus, M.J.P. van Dongen, S.S. Wijmenga, The hairpin elements of nucleic acid structure: DNA and RNA folding, Nucl. Acids Mol. Biol. 8 (1994) 56–104.
[71] T.-M. Chin, S.-B. Lin, S.-Y. Lee, M.-L. Chang, A.Y.-Y. Cheng, F.-C. Chang, et al., 'Paper-clip' type triple helix formation by 5′-d-$(TC)_3T_a(CT)_3$-$C_b(AG)_3$ (a and $b=$ 0–4) as a function of loop size with and without the pseudoisocytosine base in the hoogsten strand, Biochemistry 39 (2000) 12457–12464.
[72] L. Zhu, S.-H. Chou, J. Xu, B.R. Reid, Structure of a single-cytidine hairpin loop formed by the DNA triplet GCA, Nat. Struct. Biol. 2 (1995) 1012–1017.
[73] H.H. Ippel, H. van den Elst, G.A. van der Marel, J.H. van Boom, C. Altona, Structural similarities and differ-

ence between H1- and H2-family DNA minihairpin loops: NMR studies of octameric minihairpins, Biopolymers 46 (1998) 375–393.
[74] J. Völker, H.H. Klump, Electrostatic effects in DNA triple helices, Biochemistry 33 (1994) 13502–13508.
[75] T. Brown, G.A. Leonard, E.D. Booth, G. Kneale, Influence of pH on the conformation and stability of mismatch base-pairs in DNA, J. Mol. Biol. 212 (1990) 437–440.
[76] Y. Boulard, J.A.H. Cognet, G.V. Fazakerley, Solution structure as a function of pH of two central mismatches, C·T and C·C, in the 29 to 39 *K-ras* gene sequence, by nuclear magnetic resonance and molecular dynamics, J. Mol. Biol. 268 (1997) 331–347.
[77] N. Peyret, P.A. Seneviratne, H.T. Allawi, J.J. SantaLucia, Nearest-neighbour thermodynamics and NMR of DNA sequences with internal A·A, C·C, G·G, and T·T mismatches, Biochemistry 38 (1999) 3468–3477.
[78] M. Kouchakdjian, B.F.L. Li, P.F. Swann, D.J. Patel, Pyrimidine·pyrimidine base-pair mismatches in DNA. A nuclear magnetic resonance study of T·T pairing at neutral pH and C·C pairing at acidic pH in dodecanucleotide duplexes, J. Mol. Biol. 202 (1988) 139–155.
[79] F. Aboul-ela, D. Koh, J.r. Tinoco, F.H. Martin, Base–base mismatches. Thermodynamics of double helix formation for $dCA_3XA_3G + dCT_3YT_3G$ (X,Y = A, C, G, T), Nucl. Acids Res. 13 (1985) 4811–4824.
[80] A.G. Cornelis, J.H.J. Haasnoot, F.J. den Hartog, M. de Rooij, J.H. van Boom, A. Cornelis, Local destabilisation of a DNA double helix by a T–T wobble pair, Nature 281 (1979) 235–236.